

Bond stiffening in small nanoclusters and its consequences for mechanical and thermal properties

Raghani Pushpa, Umesh Waghmare, and Shobhana Narasimhan*

Theoretical Sciences Unit, Jawaharlal Nehru Centre for Advanced Scientific Research, Jakkur PO, Bangalore 560 064, India

(Received 21 December 2007; published 25 January 2008)

We have used density functional perturbation theory to investigate the stiffness of interatomic bonds in small clusters of Si, Sn, and Pb. As the number of atoms in a cluster is decreased, there is a marked shortening and stiffening of bonds. The competing factors of fewer but stiffer bonds in clusters result in softer elastic moduli but higher (average) frequencies as size is decreased, with clear signatures of universal scaling relationships. The stiffness of bonds is found to scale as the inverse tenth power of length. A significant role in understanding trends is played by the coordination number of the bulk structure: The higher this is, the lesser is the relative softening of elastic constants and the greater the relative damping of vibrational amplitudes for clusters compared to the bulk. Our results could provide a framework for understanding recent reports that some clusters remain solid above the bulk melting temperature. Our results suggest that Sn and Pb clusters (but not Si clusters) are more thermally stable than the bulk.

DOI: [10.1103/PhysRevB.77.045427](https://doi.org/10.1103/PhysRevB.77.045427)

PACS number(s): 63.22.-m, 61.46.Bc, 71.15.Mb

I. INTRODUCTION

With the emerging importance of nanotechnology, it has become vital to know how the mechanical strength, thermal stability, and chemical properties of very small objects compare with those of macroscopic size. These properties depend crucially on the stiffness of interatomic bonds, which determines how difficult it is to move atoms from their equilibrium positions—either in thermally induced vibrations or in response to external forces.

In this paper, we suggest, using Si, Sn, and Pb as examples, that the shortening and stiffening of bonds in small clusters may be significant enough to have a noticeable impact on elastic and thermal properties. Our calculations provide evidence of some surprising scaling relations involving the degree of bond stiffening as a function of bond lengths and coordination number. We also suggest that our results could present a framework for understanding recent experimental^{1,2} and computational³⁻⁶ reports that some clusters remain solid above the bulk melting temperature, in contradiction to a long-held belief that small objects will melt at lower temperatures than the bulk.⁷

Low-dimensional systems often display structures where the coordination number (CN) is less than in the bulk structures of the same element. From general chemical principles, one expects that such undercoordinated bonds should be shorter and stiffer; however, the extent of this stiffening is difficult to estimate accurately from simple arguments. It is important to note that a stiffening of undercoordinated bonds need not necessarily imply mechanical hardening and vibrational damping. Even if bonds become stiffer, such systems have fewer bonds per atom (compared to the bulk). Therefore, it is crucial to have a gauge of the *degree* of bond stiffening, since this will determine which of the two competing factors (of stiffer bonds but fewer bonds) will prevail, and thus decide whether or not low-dimensional systems such as nanoclusters will be softer (harder) and less (more) thermally stable than the bulk.

An enhancement in the stiffness of interatomic bonds has previously been observed in some two- and one-dimensional

systems, e.g., at the surfaces of metals,^{8,9} in thin films,¹⁰ and in nanorods and nanotubes.¹¹ Here, we investigate trends in bond stiffness as a function of size and element in zero-dimensional clusters that are small enough that their properties do not obey continuum scaling relations of the bulk and surfaces. In order to study such effects theoretically, it is crucial to have a method that can reliably reproduce the effects of changes in coordination number. Pair potentials, being insensitive to atomic coordination, are obviously inadequate, while semiempirical potentials usually have to be tailored carefully if they are to describe such many-body effects not merely qualitatively but also quantitatively. For these reasons, in this work, we choose to perform quantum mechanical density functional theory (DFT) and density functional perturbation theory (DFPT) calculations.

We have chosen Si, Sn, and Pb because we wish to demonstrate the crucial role played by the coordination number of the *bulk* structure in determining the relative properties of clusters and bulk. These three elements belong to the same column of the Periodic Table but have different bulk structures, viz., diamond, β -Sn, and face centered cubic (fcc), with CNs of 4, 6, and 12, respectively.

II. *AB INITIO* CALCULATIONS

We have studied the bulk as well as small clusters (number of atoms $N \leq 20$) of Si, Sn, and Pb using DFT and DFPT *ab initio* calculations, as implemented in the QUANTUM ESPRESSO distribution.¹² Norm conserving pseudopotentials were used, together with a plane wave basis with a cutoff of 20 Ry. Exchange and correlation effects were treated within the local density approximation (LDA) using the parametrization by Perdew and Zunger.¹³ Calculations on the bulk materials were performed for Si in the diamond structure, for Sn in the body-centered-tetragonal β -Sn phase, and for Pb in the fcc structure. We have also performed calculations for Sn in its diamond-structure α -Sn phase; however, these results are not presented in detail here, both for conciseness and relevance. The β -Sn phase makes the CN-dependent trends

more clear and is also the high-temperature phase concerned in the process of melting, the study of which was one of the motivating factors for our work. For the reciprocal space summations (k points) as well as for the wave vectors (q points) for the DFT and DFPT calculations on the bulk systems, 10, 56, 163, and 256 points in the irreducible Brillouin zone were used for Si, α -Sn, β -Sn, and Pb, respectively. Periodic boundary conditions were used, and the clusters were placed in a cubical box of side varying between 12 and 21 Å, depending on the size of the cluster; this was sufficient to remove any artificial interaction between periodic images. The equilibrium structures of clusters were obtained by starting from previously reported structures^{3,14–19} and/or regular polyhedral arrangements and relaxing using an eigenvector-following technique²⁰ that makes use of eigenvectors obtained using DFPT and Hellmann-Feynman forces.

III. RESULTS AND ANALYSIS

The clusters we have studied are tiny enough that they do not resemble bulk fragments structurally. The structures obtained by us are, for the most part, very similar to those obtained by previous authors.^{3,14–19} We have analyzed the structures by examining coordination numbers and bond lengths (interatomic spacings). We define the CN of an atom as the number of neighboring atoms that lie within a cutoff distance R_c ; we have verified that the trends presented in the rest of this paper are not sensitive to the precise choice of R_c . The mean CN of the cluster is then obtained by averaging over all the atoms. In Figs. 1(a) and 1(b), we show how $\langle C \rangle$, the average CN, and $\langle L \rangle$, the average bond length, vary with N , the number of atoms in the cluster. We find that both $\langle C \rangle$ and $\langle L \rangle$ indeed decrease (as expected) as N becomes smaller. The shortening of bond lengths is particularly marked for such small clusters, where all atoms are essentially surface atoms, and bonds can contract freely, as there is no need to maintain registry with a bulklike core; this is not true, e.g., for near-surface bonds at low-index faces of single crystals. It is also noteworthy that the clusters of the three elements display very similar structures, despite the diverse nature of the three bulk phases; this may possibly be due to a transition from metallic to covalent bonding at small cluster sizes, as has been suggested for Ga.²¹

In Fig. 1(a), note that the dashed line representing the bulk CN is positioned differently relative to the curve of $\langle C \rangle$ vs N for the three cases: for Pb, the former lies well above the latter; for β -Sn, the former lies slightly above the latter; whereas for Si, that $\langle C \rangle$ is smaller in the cluster than in the bulk is true only for $N \leq 6$. This is of course a simple corollary of the three different bulk structures of Si, β -Sn, and Pb; however, its consequences are consistently manifested in three different kinds of behavior of the clusters relative to the corresponding bulk, as we will demonstrate below. For example, in Fig. 1(b), we see that the average bond length for most Sn (Pb) clusters is less (much less) than the nearest-neighbor bond length in the bulk, but for Si, this is true only up to $N=5$.

Next, we use DFPT (Ref. 22) to compute the interatomic force constant tensors (IFCTs), vibrational frequencies, and

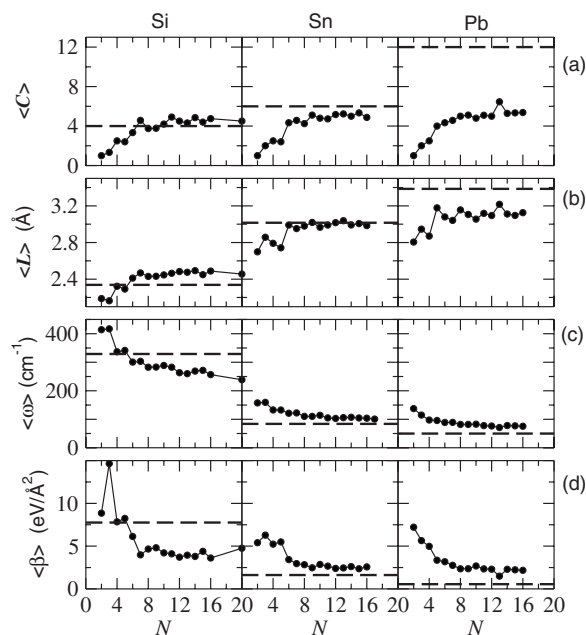


FIG. 1. Smaller clusters have, on average, lower coordination, shorter and stiffer bonds, and higher frequencies. The dots show how the average (a) coordination number $\langle C \rangle$, (b) bond length $\langle L \rangle$, (c) vibrational frequency $\langle \omega \rangle$, and (d) radial force constant $\langle \beta \rangle$ vary with N , the number of atoms in the cluster. The dashed horizontal lines indicate the corresponding values for bulk Si, β -Sn, and Pb; note that these lines are positioned differently with respect to the dots for the three elements.

eigenvectors for all the clusters, as well as for the bulk structures. We emphasize that this is an exact but computationally efficient procedure, involving no fitting or assumptions about the range or form of interatomic interactions or about the directions of eigenvectors. Once again, clusters of the three elements behave differently vis-à-vis the bulk: We find that Sn and Pb clusters have vibrational frequencies that lie above ω_{max}^b , the highest phonon frequency of the bulk; however, this is not true for Si clusters (with the exception of $N=3$ and $N=20$). As an example, we present the vibrational spectrum for ten-atom clusters of Si, Sn, and Pb in Fig. 2, as well as the corresponding bulk phonon density of states. Note that

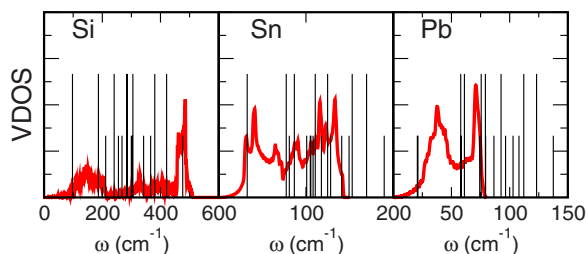


FIG. 2. (Color online) DFPT results for the vibrational spectra of clusters and bulk. The thin vertical black lines indicate the vibrational density of states (VDOS) for ten-atom clusters of Si, Sn, and Pb, while the thick curves (red) indicate the phonon density of states for the corresponding bulk material. The highest frequency for the bulk is lower than that of the cluster for Sn and Pb (but not for Si).

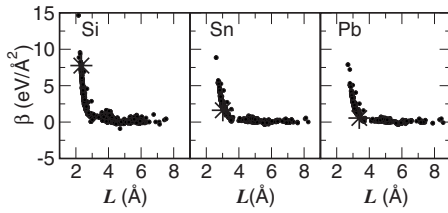


FIG. 3. The black dots show our results for the radial force constant β versus bond length L . Note that the data for each element collapse onto a smooth graph. The stars represent the data for the nearest-neighbor bonds in the bulk structure; one can see clearly that bonds in bulk Si (but not in Sn and Pb) are stiffer than bonds in the clusters. These graphs contain the data for all pairs of atoms in all the clusters, corresponding to 870, 675, and 680 data points for Si, Sn, and Pb, respectively.

the highest frequency mode for Sn_{10} and Pb_{10} exceeds ω_{max}^b by 32% and 73%, respectively, whereas for Si_{10} , it is lower by 7%.

In order to display trends more clearly, we fit the (exact) IFCTs to a sum of pairwise radial and tangential terms. By assembling the results for all pairs of atoms for all sizes of clusters, we have, in this way, obtained a very large number of results for radial force constants β as a function of bond lengths L (depicted in Fig. 3). We find that β varies rather smoothly as the inverse tenth power of L for all three elements. We are not aware of any simple explanation for the origin of this power law behavior, and further work needs to be done to examine this issue and to check whether or not it is applicable also to other elements. We also wish to stress that though the values of β presented here do involve an approximation of the form of the interatomic interactions, they are presented here primarily as a convenient way to display trends; subsequent results for vibrational frequencies and displacements (presented below) are obtained using the exact IFCTs and not the approximate β .

The average size-dependent behavior of force constants and frequencies is shown in Figs. 1(c) and 1(d). We find that the average vibrational frequency $\langle\omega\rangle$ and average radial force constant $\langle\beta\rangle$ increase as N is decreased. Note again the three different kinds of behavior relative to the bulk: in this size range, clusters of Sn and Pb (but not Si) have stiffer bonds and higher vibrational frequencies (on average) than the corresponding bulk. It is also clear on examining the panels of Fig. 1 that the size of the cluster below which bonds become stiffer in the cluster than in the bulk is effectively determined by the coordination number of the bulk structure.

Though the Sn and Pb clusters have stiffer bonds than the corresponding bulk [see Fig. 1(d)], there are fewer such bonds per atom [see Fig. 1(a)]. These two effects compete in determining the elastic and thermal properties. We find that the latter effect dominates when we compute the elastic modulus for dilation, which serves as a measure of hardness and is defined as $c_d = \frac{1}{N} \partial^2 E / \partial \delta^2$, where E is the total energy of the system consisting of N atoms, which has been dilated or compressed by a factor $(1 + \delta)$; for the clusters, the dilation was carried out about the center of mass. This definition of

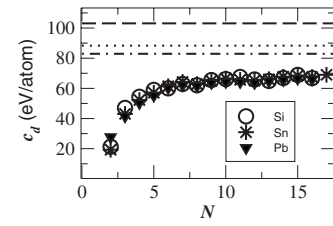


FIG. 4. Size dependence of the elastic modulus for dilation, c_d . N is the number of atoms in the cluster. The open circles, stars, and filled triangles are the data for Si, Sn, and Pb clusters, respectively, while the dashed, dotted, and dot-dashed lines represent the results for bulk Si, β -Sn, and Pb, respectively. Note that the clusters are softer than the bulk, and the data for clusters of the three elements appear to collapse onto a single curve.

an elastic modulus may appear somewhat unfamiliar; note that it has dimensions of energy. We believe this to be appropriate for zero-dimensional objects such as clusters, as an extension of the fact that elastic moduli for three-, two-, and one-dimensional objects are traditionally defined as having dimensions of energy/(length)³, energy/(length)², and energy/length, respectively. It also has two further advantages: (i) It sidesteps the need to define the volume of a cluster (various formulations for defining the volume of a nanosystem have been used in the literature, and we find that the volume obtained can vary considerably upon the definition used, thus making any evaluation of elastic moduli that incorporate definitions of volumes highly open to ambiguity). (ii) The definition of c_d used by us permits a direct comparison between the cluster and the bulk, as c_d can also be precisely defined for a bulk system, with, in this case, all bond lengths being scaled by a factor of $(1 + \delta)$. In Fig. 4, we show how c_d varies with N . As the size of the cluster is increased, we find that c_d increases; while these curves will presumably approach the bulk values (horizontal lines) for very large sizes, we are well below the regime where this occurs. An unexpected and striking feature of this graph is the data collapse for all but the smallest cluster sizes. For a given N , the value of c_d is the same for all three elements; this is not true, however, for the bulk elements. We find that this data collapse results from a scaling relation such that, for a given CN , the bond stiffness multiplied by the square of the bond length is approximately the same for all three elements. Note also that while all the clusters are softer than the corresponding bulk, Pb clusters are hardest *relative to the bulk* and Si clusters are the softest, in agreement with the trends observed above.

The enhanced bond stiffness competes with the lesser number of bonds also in determining the mean squared displacements (MSDs) of atoms; however, we find that in this case, it is the former and not the latter that wins out. Within the harmonic approximation, the MSD of the i th atom in the cluster and/or bulk at temperature T is given by:²³

$$\langle u_i^2(T) \rangle = \frac{1}{N_{\mathbf{k} \mathbf{k} \lambda \alpha}} \sum_{\mathbf{k} \mathbf{k} \lambda \alpha} \frac{\hbar}{M \omega_{\mathbf{k} \lambda}} |e_{\mathbf{k} \lambda}^{i \alpha}|^2 \left(n_{\mathbf{k} \lambda} + \frac{1}{2} \right), \quad (1)$$

where the vibrational frequencies $\omega_{\mathbf{k} \lambda}$ and eigenvectors $e_{\mathbf{k} \lambda}^{i \alpha}$ are known from DFPT; \mathbf{k} denotes the phonon wave vector

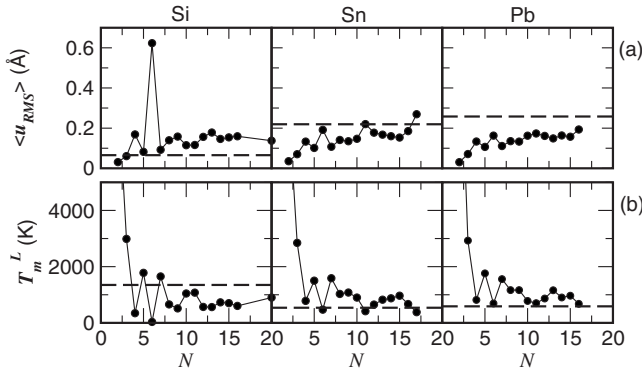


FIG. 5. Trends and oscillations in vibrational amplitudes and melting temperatures: $\langle u_{rms} \rangle$ is the root-mean-squared displacement at 300 K, averaged over all the N atoms of the cluster, and T_m^L is the Lindemann estimate of the melting temperature. The dots and dashed lines are the calculated values for the clusters and bulk, respectively. Note that for Sn and Pb (but not Si), the dots lie below (above) the dashed line in the upper (lower) panel.

($\mathbf{k}=0$ for all cluster modes), $N_{\mathbf{k}}$ is the number of wave vectors in the Brillouin zone, λ runs over all modes at a given \mathbf{k} , α specifies Cartesian directions, M is the atomic mass, \hbar is Planck's constant, and $n_{\mathbf{k}\lambda}$ is the temperature-dependent Bose-Einstein occupation factor. We find that, for a given temperature T , (i) though there is some variation in the MSDs among the different atoms in a cluster, there is an overall trend toward smaller MSDs as the cluster size decreases [see Fig. 5(a)]; (ii) this variation is, however, non-monotonic; (iii) the MSDs for most Sn and Pb (but not Si) clusters are smaller than for the bulk. This is in contrast to what is observed at the low-index surfaces of single crystals, where, though the undercoordination of surface atoms leads to an enhancement in some force constants,^{8,9} the MSDs at the surface are still larger than in the bulk.^{9,24}

Finally, we investigate the possible implications of our results for the melting behavior of clusters. The conventional argument has been that surface atoms have fewer neighbors than bulklike atoms, and are therefore less constrained, resulting in greater amplitudes of thermal vibration and lower melting temperatures. This is in accordance with the frequently observed phenomenon of premelting at flat surfaces of single crystals²⁵ and would suggest that clusters (with their large surface-to-volume ratio) should melt at lower temperatures than the bulk. This view was supported by early experiments and molecular-dynamics simulations on the melting of clusters.²⁶ However, the majority of these simulations used pair potentials, e.g., Morse or Lennard-Jones,^{26,27} and thus cannot incorporate any effect of bond stiffening. Moreover, recent experiments on size-selected clusters of Sn and Ga suggested that some clusters melt at temperatures above the bulk melting temperature.^{1,2} These experiments were initially motivated³ and later confirmed⁴⁻⁶ by *ab initio* molecular-dynamics simulations, which showed that certain clusters of Sn and Ga are solid above the bulk melting temperature T_m^b . However, it has not been clear whether such results hold only for sizes corresponding to particularly stable atomic arrangements and whether they can be extended to other elements.

As a rough indicator of the consequences of bond stiffening on melting behavior, we have computed the Lindemann melting temperature T_m^L using a generalized form²⁷ of the Lindemann criterion, which states that objects melt when vibrational amplitudes become equal to a critical fraction Δ of interatomic distances:

$$\Delta = \frac{1}{N_b} \sum_{|r_{ij}| < R_c} \frac{\{\langle u_i^2 \rangle + \langle u_j^2 \rangle - 2\langle u_i u_j \rangle\}^{1/2}}{\langle r_{ij} \rangle}. \quad (2)$$

Here, $\langle r_{ij} \rangle$ is the mean value of the distance between atoms i and j , and N_b is the number of bonds shorter than the cutoff distance R_c . We have chosen $\Delta=0.13$; though the precise numerical results depend on this choice, we have verified that the trends displayed are robust. We first computed T_m^L for the bulk phases [dashed lines in Fig. 5(b)] obtaining values of 1350, 537, and 588 K for Si, β -Sn, and Pb, respectively, in fairly good agreement with the experimental melting temperatures of 1680, 505, and 600 K. The underestimation of T_m^b for Si is a well-known feature of the LDA, and our estimate is in excellent agreement with the result obtained using a more sophisticated treatment.²⁸

The dots in Fig. 5(b) show our results for T_m^L for clusters as a function of N . (This is only an approximate indicator of melting temperature, both because of the empirical nature of the Lindemann criterion and because of the broad nature of the melting transition in finite-sized systems. Moreover, in some clusters, the melting temperature may be preempted by fragmentation.²⁹) From Fig. 5(b), we see that huge oscillations are superposed on an overall trend where T_m^L increases as N decreases.

The trends we have observed for the clusters relative to the bulk are maintained here, too [compare the dots and dashed lines in Fig. 5(b)]; i.e., for Sn (Pb), most (all) clusters in this size regime have T_m^L above that of the bulk, whereas for Si, the majority of clusters have T_m^L below the bulk. For Sn, this is in qualitative agreement with experimental and computational findings,¹⁻⁶ while we offer our results of enhanced melting temperatures for Pb clusters as a prediction awaiting experimental validation.

The puzzling oscillations in Fig. 5(b) are reminiscent of those observed in the size dependence of the melting temperature of Na clusters,⁷ which could not be explained by either geometric or electronic shell closing arguments. We find that these oscillations in T_m^L result primarily from oscillations in the value of the lowest vibrational frequency ω_{min} . As an example, in Fig. 6, we present the results for the size dependence of both ω_{min} and T_m^L for Sn clusters. Unlike $\langle \omega \rangle$, ω_{min} varies nonmonotonically with N , is very sensitive to the exact structure, and reflects variations in tangential force constants. It is clear from Fig. 6 that the oscillations in the lowest nonzero frequency are reflected in the Lindemann melting temperatures. A similar effect is also observed for Si and Pb clusters.

IV. SUMMARY AND CONCLUSIONS

In summary, we have computed the structure and vibrational properties of clusters and bulk of Si, Sn, and Pb, and

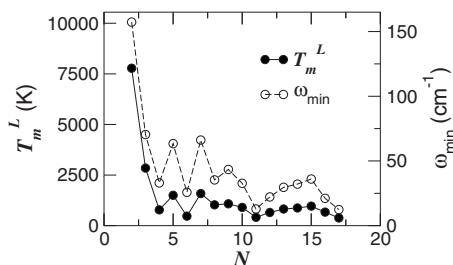


FIG. 6. The oscillations in the Lindemann melting temperature reflect those in the value of the lowest vibrational frequency. The filled and open circles represent, respectively, the data for T_m^L and ω_{min} for Sn clusters as a function of the number of atoms N in the cluster.

shown the presence of clear size-dependent trends. We have found that for Sn and Pb, bonds in clusters are shorter and stiffer than in the bulk, and this, in turn, suggests that small clusters of Sn and Pb melt at higher temperatures than in the bulk; for Sn, this is in agreement with previous experiments and molecular-dynamics simulations. However, for Si, we find that the bonds in clusters are slightly longer and softer than in the bulk, and that Si clusters melt at temperatures below the bulk.

Interestingly, we find that if the comparison for Sn clusters were to be made not with β -Sn but with the low-temperature phase of diamond-structure α -Sn (which, in reality, transforms to β -Sn before it melts), the behavior of Sn would be similar to that of Si, i.e., the clusters would have lower vibrational frequencies and softer bonds and melt at lower temperatures than the bulk.

We have also found evidence for two scaling relations: (i) the stiffness of a bond scales as the inverse tenth power of the bond length and (ii) the elastic modulus for dilation (defined in the previous section) depends on size but not on element for Si, Sn, and Pb. At present, we do not have a complete understanding of where these relations arise from; further work in this regard is in progress.

The main approximation made in our work and analysis is the use of the empirical Lindemann criterion as a gauge of melting temperatures. The melting temperature is anyway not precisely defined for finite systems which do not display a sharp transition; typically, in calorimetric experiments and molecular-dynamics simulations, the melting temperature is given as the temperature where the specific heat capacity reaches a maximum. While we do not, therefore, place too

much weight on our numerical values of T_m^L , we do believe that they serve as a good indicator of comparative trends for size and element dependence and for the behavior of clusters relative to the bulk. The broad specific heat curves seen in experiments and simulations also contain information about structural transitions between various low-lying isomers. Transitions between these local minima in the energy landscape are controlled at lowest order by the stiffness of the basins, i.e., the frequencies of vibrational modes. Since the CN does not, typically, vary significantly among these low-lying isomers, our general arguments should prevail also if one defines melting as a transition between various metastable configurations (rather than a transition from the liquid to the solid state) and if one accounts for the fact that at finite temperatures, even monodisperse clusters may display a variety of structural configurations.

Our work also provides an explanation for the puzzling oscillations observed in the size dependence of the melting curves for clusters.⁷ We suggest that a low melting temperature correlates with the presence of a soft vibrational mode for a cluster; note that this also implies the presence of a low-energy route for structural isomerization.

Most of the trends displayed in this paper are shown to track along with changes in coordination number. It is noteworthy that this seems to apply to both metallic and covalently bonded systems. The results and analysis presented above suggest persuasively that the differences (in the comparative behavior of clusters and bulk) between Si, Sn, and Pb can be attributed to differences in bulk structure; our arguments are general enough that we believe they should be valid for a variety of elements. Our results lead to the following rules of thumb: The larger the coordination number in the bulk, the less the relative softening in the elastic moduli of small clusters and the more likely it is that such small clusters are stable at temperatures above that where the bulk melts. In accordance with this understanding, we note that a very recent molecular-dynamics simulation³⁰ suggests that Au clusters have a melting temperature above that of bulk (fcc) gold.

ACKNOWLEDGMENTS

Funding was provided by DST. S.N. acknowledges the hospitality of the Department of Chemistry, University of Cambridge, where a part of this work was performed. Helpful conversations with Dilip Kanhere, David King, Michele Parrinello, and David Wales are gratefully acknowledged.

*shobhana@jncasr.ac.in

¹A. A. Shvartsburg and M. F. Jarrold, Phys. Rev. Lett. **85**, 2530 (2000).

²G. A. Breaux, R. C. Benirschke, T. Sugai, B. S. Kinnear, and M. F. Jarrold, Phys. Rev. Lett. **91**, 215508 (2003).

³Z.-Y. Lu, C.-Z. Wang, and K.-M. Ho, Phys. Rev. B **61**, 2329 (2000).

⁴K. Joshi, D. G. Kanhere, and S. A. Blundell, Phys. Rev. B **66**,

155329 (2002).

⁵K. Joshi, D. G. Kanhere, and S. A. Blundell, Phys. Rev. B **67**, 235413 (2003).

⁶F. C. Chuang, C. Z. Wang, S. Ögüt, J. R. Chelikowsky, and K. M. Ho, Phys. Rev. B **69**, 165408 (2004).

⁷M. Schmidt, R. Kusche, B. von Issendorff, and H. Haberland, Nature (London) **393**, 238 (1998).

⁸K. M. Ho and K. P. Bohnen, Phys. Rev. Lett. **56**, 934 (1986).

- ⁹S. Narasimhan, Phys. Rev. B **64**, 125409 (2001).
- ¹⁰A. Sirenko, C. Bernhard, A. Golnik, A. Clark, J. Hao, W. Si, and X. Xi, Nature (London) **404**, 373 (2000).
- ¹¹E. Wong, P. Sheehan, and C. Lieber, Science **277**, 1971 (1997).
- ¹²S. Baroni, S. de Gironcoli, A. Dal Corso, and P. Giannozzi, <http://www.quantum-espresso.org>
- ¹³J. P. Perdew and A. Zunger, Phys. Rev. B **23**, 5048 (1981).
- ¹⁴P. Ballone, W. Andreoni, R. Car, and M. Parrinello, Phys. Rev. Lett. **60**, 271 (1988).
- ¹⁵K. Raghavachari and C. M. Rohlfing, J. Chem. Phys. **89**, 2219 (1988).
- ¹⁶K. M. Ho, A. A. Shvartsburg, B. Pan, Z. Y. Lu, C. Z. Wang, J. G. Wacker, J. L. Fye, and M. F. Jarrold, Nature (London) **392**, 582 (1998).
- ¹⁷B. X. Li and P. L. Cao, Phys. Rev. B **62**, 15788 (2000).
- ¹⁸C. Majumder, V. Kumar, H. Mizuseki, and Y. Kawazoe, Phys. Rev. B **64**, 233405 (2001).
- ¹⁹J. P. K. Doye, Comput. Mater. Sci. **35**, 227 (2006).
- ²⁰R. Pushpa, S. Narasimhan, and U. Waghmare, J. Chem. Phys. **121**, 5211 (2004).
- ²¹S. Chacko, K. Joshi, and D. G. Kanhere, Phys. Rev. Lett. **92**, 135506 (2004).
- ²²S. Baroni, S. de Gironcoli, A. Dal Corso, and P. Giannozzi, Rev. Mod. Phys. **73**, 515 (2001).
- ²³R. E. Allen and F. W. de Wette, Phys. Rev. **179**, 873 (1969).
- ²⁴S. Narasimhan, Surf. Sci. **496**, 331 (2002).
- ²⁵H. Dosch, *Critical Phenomena at Surfaces and Interfaces* (Springer, Berlin, 1992).
- ²⁶D. Wales, *Energy Landscapes: Applications to Clusters, Biomolecules and Glasses* (Cambridge University Press, Cambridge, 2004).
- ²⁷Y. Zhou, M. Karplus, K. D. Ball, and R. S. Berry, J. Chem. Phys. **116**, 2323 (2002).
- ²⁸O. Sugino and R. Car, Phys. Rev. Lett. **74**, 1823 (1995).
- ²⁹G. A. Breaux, C. M. Neal, B. Cao, and M. F. Jarrold, Phys. Rev. B **71**, 073410 (2005).
- ³⁰B. Soulé de Bas, M. Ford, and M. Cortie, J. Phys.: Condens. Matter **18**, 55 (2006).